THE JOURNAL OF PHYSICAL CHEMISTRY C

Feature Article

pubs.acs.org/JPCC

Interpretation of Diffusion and Recombination in Nanostructured and Energy-Disordered Materials by Stochastic Quasiequilibrium Simulation

Mehdi Ansari-Rad,[†] Juan A. Anta,*[,‡] and Juan Bisquert*[,§]

[†]Department of Physics, University of Tehran, 1439955961 Tehran, Iran

[‡]Área de Química Física, Departamento de Sistemas Físicos, Químicos y Naturales, Universidad Pablo de Olavide, E-41013 Sevilla, Spain

[§]Grup de Dispositius Fotovoltaics i Optotlectrònics, Departament de Física, Universitat Jaume I, 12071 Castelló, Spain

ABSTRACT: The main electronic feature of many nanocrystalline semiconductors and organic materials is the presence of a distribution of localized states in the system with a broad energy dispersion. Carrier transport and recombination in these energetically disordered systems have raised increasing attention, in relation to applications in novel optoelectronic devices. We provide a general view of the physical interpretation of carrier transport coefficients (diffusion coefficient and mobility) and recombination lifetime in the presence of the localized states. We aim to carefully distinguish between the quantities that appear in the continuity equation for a small perturbation of the charge carriers (collective diffusion coefficient and lifetime) and those that are related to the behavior of the individual carriers (single-particle quantities). As an important example, charge-carrier transport and recombination in the case of multiple trapping model will be discussed in detail, for both exponential and Gaussian distributions. We address important aspects of the interpretation of lifetime and charge-transfer rates related to recombination in nanostructured organic and hybrid solar cells. Finally, to clarify different definitions for diffusion coefficient and lifetime, we use Monte Carlo simulation to calculate the diffusion coefficient, the mobility, and the lifetime (for both linear and nonlinear recombination) in the Gaussian DOS. We also justify the validity of the generalized Einstein relation in the case of a non-Boltzmann distribution of the carriers. Definitions and calculations provided in this paper have important consequences for both the interpretation of measurements and the calculation with advanced transport and recombination models.

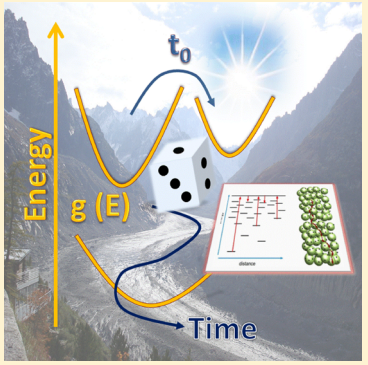

1. INTRODUCTION

Organic semiconductors, conductive small molecules, and nanostructured metal-oxide semiconductors are new classes of disordered materials that have received considerable interest from science and technology in recent years. Optoelectronic devices such as dye-sensitized solar cells (DSCs),[1] organic solar cells,[2] and organic light-emitting diodes (OLEDs)[3] are examples showing the wide applications of these materials. Inherent morphological and structural disorder of these materials leads to energetically disordered systems. The fundamental feature of such systems is that, aside from (or, instead of) extended states, there is a distribution of localized states in the material in contrast with crystalline semiconductors.

Transport and recombination of charge carriers in the presence of localized states with an intrinsic energy disorder[4,5] is the main subject of this paper. New physical insights into the interpretation of the experimental observations for transport coefficients have recently been provided for nanocrystalline semiconductors and organic materials.[6] Because of the complexity of phenomena in such systems, a detailed understanding of the mechanism of charge transport and recombination in disordered materials is still an active field of research (especially in the case of organic polymers). For the same reason, interpretation of the measured quantities has remained an important problem that needs a deeper investigation.[7,8] Section 2 is devoted to carefully defining the various quantities that characterize transport and recombination of the charge carriers in the materials with distribution of localized states. These definitions are valid for both organic and inorganic materials, irrespective of the underlying mechanism of transport and recombination.

When there is a broad distribution of localized states in the material, most charge carriers injected into the system are permanently localized. Two main approaches have been used to explain charge-carrier transport in this situation. The first is the multiple trapping (MT) model. In this model, transport occurs by carrier jumps to a band of extended states (above the mobility edge) wherein carriers are free to move. MT has been a successful model to explain the transport properties in the metal-oxide semiconductors used in DSCs.[9] In Sections 3.1 and 3.2 we will focus on this model and discuss general features of

Received: April 1, 2013
Revised: May 14, 2013
Published: June 10, 2013

   dx.doi.org/10.1021/jp403232b | J. Phys. Chem. C 2013, 117, 16275−16289

the transport and recombination. The second approach is the hopping transport model.[10] Unlike the MT model, in which transport occurs by thermal activation of the localized carriers to extended states, in the case of hopping transport, direct transition between localized states takes place. This transition occurs via a combination of thermal activation and quantum mechanical tunneling. The hopping model is widely used to describe the transport properties in the organic semiconductors wherein there is not any extended state in the system. However, in some situations, especially when the carriers are situated deep energetically in the tail of the energy distribution, hopping transport leads to the same behavior of the transport coefficients as that predicted by the MT model. In fact, it has been shown that in the hopping transport there is a particular level, called transport energy, that determines the dominant hopping events. This level plays the same role as the mobility edge in the MT model. (See refs 11−15.) We briefly discuss this issue in Section 3.

Apart from the somewhat different mechanism of carrier transport between nanostructured metal oxides and organic semiconductors, the form of the density of states (DOS) is also different between these two classes of materials. The common exponential DOS below the conduction band that merges with the extended states is usually seen in the metal-oxide semiconductors, for example, TiO_2[16,17] or ZnO[18,19] nanostructures in DSCs. The Gaussian DOS is usually observed in conductive polymers.[20] In Sections 3.3 and 3.4 we will investigate MT transport and recombination in both of these distributions.

Monte Carlo simulation (also called random walk numerical simulation) is a natural way to investigate the electronic process in disordered systems that we are interested in.[21−23] In fact, the nature of the transport and the recombination in disordered materials is quite stochastic, so that the use of the Monte Carlo method is especially well-suited to study the behavior of these systems from "first-principles" with a reasonable numerical demand. As we aim to describe the system based on microscopic assumptions before the simulation, one has to decide about the model of transport and recombination. At the next step, Monte Carlo methods can be used to simulate the transport and the recombination processes and then test if the microscopic models used are capable of reproducing the experimental behavior. In Section 3.4, using this powerful tool, we test the general definitions of Section 2 for the transport and recombination in the case of the Gaussian DOS. In addition to the energetics, morphology of the semiconductor material is also a determining factor in the behavior of the system. Monte Carlo method is also useful to investigate the morphological disorder; however, it is not the purpose of the present paper to consider this kind of disorder. We refer the reader to several papers in this subject that cover different aspects of this problem in the field of DSCs.[24−27]

Of great importance in semiconductors is the connection between the diffusion and drift coefficients. Diffusion-to-mobility ratio, in its classical form, is known as Einstein relation. Although it was known[28−32] that this classical statement has limitations and holds only under Boltzmann statistics (see Section 2.2), it was in the field of disordered materials that the deviation from the classical form attracted much attention.[33−35] Description of this deviation, known as generalized Einstein relation, was first applied by Roichman and Tessler in disordered organic conductors.[36] However, it has recently been argued that under quasiequilibrium conditions classical Einstein relation is always fulfilled in disordered organic semiconductors.[37] In Section 3.4, using Monte Carlo simulation, we will show that in the presence of the localized states, as long as the distribution of the carrier deviates from the Boltzmann statistics, it is the generalized Einstein relation that gives the correct value for diffusion-to-mobility ratio in the equilibrium conditions.

2. TRANSPORT COEFFICIENTS AND LIFETIME

In this section we briefly discuss transport and recombination in the disordered electronic systems. We do not limit ourselves to a particular mechanism for the transport or recombination. Instead, we propose some general definitions for both the transport coefficient and the recombination lifetime. The main message of our discussion will be the difference between the jump quantities and the collective quantities. The former are the quantities that describe the motion of the individual carriers and can directly be probed in the stochastic simulation. The latter are the parameters that appear in measurements based on a small perturbation of carrier population and correspond to the natural kinetic coefficients in the continuity equation for density of carriers often used to model systems and devices.

2.1. Quasiequilibrium Condition and the Small Perturbation Idea. Consider a system of electronic species with density n. Assuming a DOS function, $g(E)$, the carrier density is given by (note that here $g(E)$ is the *total* DOS, including both the localized and the extended states)

$$n = \int g(E) f(E - E_F)\, dE \tag{1}$$

where $f(E - E_F)$ is the Fermi−Dirac distribution function

$$f(E - E_F) = \frac{1}{1 + \exp\left(\frac{E - E_F}{k_B T}\right)} \tag{2}$$

where k_B is Boltzmann's constant and T is the absolute temperature. E_F is the electrochemical potential (or Fermi level) of the carriers and is composed of two parts: the electric potential $-q\varphi$ and the chemical potential μ[38]

$$E_F = -q\varphi + \mu \tag{3}$$

where q is the positive elementary charge.

Equation 1 in fact assumes that the system is under equilibrium, or at least, *quasiequilibrium* conditions. Here equilibrium means that the carriers in all states of the distribution are thermalized to a *steady-state* Fermi level. Now, suppose that we want to measure some kinetic properties of the system, for example, transport coefficient or lifetime of the carriers. This necessarily requires us to monitor the evolution of a modification of the system. The way to do this is to perturb the equilibrium state by injecting some excess carriers into the system and then measuring the transit time for recovery of the initial equilibrium state or, alternatively, to determine the response to a periodic perturbation of some quantity. Although there is not a steady-state Fermi level during the transit time or oscillation measurements, we assume that there is still a *well-defined* stationary Fermi level in the system, which is time-independent, with respect to the monitored kinetics. This is the quasiequilibrium approximation that allows us to measure specific kinetic coefficients because the coefficient can be attributed to the specific state fixed by the given stationary Fermi level. In practice a small voltage modulation as in impedance spectroscopy or a time-dependent

dx.doi.org/10.1021/jp403232b | J. Phys. Chem. C 2013, 117, 16275−16289

light intensity perturbation as in time-transient spectroscopies can be neatly separated from the system's steady state that determined the constant Fermi level. Additionally, we consider only homogeneous conditions in which the Fermi level does not depend on the position. (Such a situation can readily be established in solar cells at open circuit.)

As will be discussed in the following sections, in disordered materials, both the transport coefficient and the lifetime are strong functions of the carrier density. Therefore, the system should only slightly be perturbed from the equilibrium state (i) to stay near the equilibrium concentration and (ii) to obtain a meaningful value of the transport coefficient and the lifetime. Therefore, we usually employ the term "small perturbation" for the transport coefficient or lifetime to emphasize that they are (should be) measured by small perturbation techniques. In fact the small perturbation idea reduces the complicated continuity equation for total carriers to a simple continuity equation for the excess carriers. This, in turn, simplifies the interpretation of the experimental results. Small perturbation techniques are widely used in the field of DSCs. (For recent reviews, see refs 39 and 40.)

In summary, the quasiequilibrium measurement or simulation makes reference to a well-defined stationary Fermi level during kinetic evolution. In contrast, quasistatic condition, further discussed below, means that all electronic states in the distribution have a common Fermi level due to fast equilibration between the different types of states.

2.2. Transport Coefficients. From the macroscopic point of view, and in the absence of a temperature gradient, the driving force for an electronic species is given by the gradient of its electrochemical potential. On the basis of the Onsager reciprocity theorem, and in the linear approximation, the carrier flux and the driving force are proportional, as[41]

$$J_n = -\frac{nu_n}{q}\frac{\partial E_F}{\partial x} \tag{4}$$

where u_n is a phenomenological coefficient called *mobility* (x is an arbitrary space coordinate). The mobility can be defined on the basis of the difference of effective charge carrier jump probability in the direction along and against the electric field. (See Section 3.4.)

As discussed above, for a system of weakly interacting particles, the electrochemical potential in eq 4 is the sum of the electric potential and the chemical potential. In the absence of an electric potential gradient and when the chemical potential is nonuniform, we have a pure *diffusion* current

$$J_n = -\frac{nu_n}{q}\frac{\partial \mu}{\partial x} \tag{5}$$

Diffusion is also formulated in terms of the concentration gradient in Fick's form

$$J_n = -D_n\frac{\partial n}{\partial x} \tag{6}$$

The coefficient D_n in eq 6 is called the *chemical* or collective diffusion coefficient. In measurements of diffusion in devices and materials, a small gradient of the concentration is induced and the correspondent flux is determined,[42] which leads to the measurement of the chemical diffusion coefficient. Now, if we compare eq 5 with eq 6, we will find the so-called *generalized Einstein relation*

$$\frac{D_n}{u_n} = \frac{k_BT}{q}\chi_n \tag{7}$$

where χ_n is called the *thermodynamic factor* and is defined as

$$\chi_n = \frac{n}{k_BT}\frac{\partial \mu}{\partial n} \tag{8}$$

We note that $f(E - E_F)$ reduces to the Boltzmann distribution, $\exp((E_F - E)/k_BT)$, when $E - E_F \gg k_BT$. With the Boltzmann distribution, irrespective of the form of DOS in eq 1, n depends exponentially on μ/k_BT, and as a result we will have χ_n =1. In this case, we obtain the *classical Einstein relation*, that is

$$\frac{D_n}{u_n} = \frac{k_BT}{q} \tag{9}$$

However, it is easy to show that, in general $\chi_n \geq 1$. The thermodynamic factor contains the effect of the interactions among the carriers, which cause $\chi_n > 1$. (See refs 6 and 43 for several examples and also Figure 3.) It is useful to make connections with important quantities in general physical chemistry. As a matter of fact, the thermodynamic factor is related to the *activity coefficient* γ of carriers, defined via $a = \gamma n$ and $\mu = \mu^{ideal} + k_BT \ln a$, where a is the activity.[44] It can be shown easily that $\chi_n = 1 + d \ln(\gamma)/d \ln(n)$.[45] An ideal, noninteracting system, characterized by $\gamma = 1$, or an activity coefficient independent of density leads to χ_n =1. This is the analogous situation to the case in which n depends exponentially on μ/k_BT, as mentioned above.

The thermodynamic nature of D_n makes it necessary to relate it to individual properties of the carriers. To this end, let us first introduce the *jump* diffusion coefficient for a d-dimensional space as

$$D_J = \frac{1}{2dt}\left\langle \frac{1}{N}\left(\sum_{i=1}^{N}\Delta r_i\right)^2 \right\rangle \tag{10}$$

Here Δr_i is the displacement of the ith particle at time t and $\langle\rangle$ denotes a statistical average. More precisely, the jump diffusion coefficient defined by eq 10 reflects a random walk of the center of mass of N particles. The relation between the jump and the chemical diffusion coefficient is given by[46,47]

$$D_n = \chi_n D_J \tag{11}$$

Now, using eqs 7 and 11, for the generalized Einstein relation we can get[48]

$$\frac{D_J}{u_n} = \frac{k_BT}{q} \tag{12}$$

Equation 12 is *generally valid* under quasiequilibrium conditions and has the form of the classical Einstein relationship eq 9. However, D_J is not the coefficient appearing in Fick's law, eq 6. The difference between jump and kinetic diffusion coefficient has clearly been demonstrated in the work by van de Lagemaat et al.[49]

If we can follow the diffusive motion of each individual particle, the so-called *tracer* (or *single-particle*) diffusion coefficient will be a relevant parameter, defined as[46,47]

$$D^* = \frac{1}{2dNt}\left\langle \sum_{i=1}^{N}(\Delta r_i)^2 \right\rangle \tag{13}$$

dx.doi.org/10.1021/jp403232b | J. Phys. Chem. C 2013, 117, 16275−16289

In fact, in the numerical evaluation of diffusion coefficients, for example, through the Monte Carlo or molecular dynamics simulations, it is D^* that is usually computed. If, on average, there are no cross correlations between displacements $\Delta r_i(t)$ of different particles at different times, then D^* and D_J become equivalent.[43,47] In the following, we will assume that the jump and the single-particle coefficients are the same. This condition is obtained if carriers do not interact significantly with each other, which is a reasonable assumption for the systems of interest here.

As previously mentioned, in the experimental methods usually a gradient of the concentration is established, and thus the quantity that is usually measured in the experiment is D_n and not D_J. However, eq 12 suggests that, by measuring the mobility, one can directly achieve the jump diffusion coefficient D_J.

2.3. General Definitions for Lifetime. We now consider the recombination of carriers. Traditional recombination addresses the process of annihilation of electrons and holes in a single material. In disordered and multiple-phase nanostructured materials, it is usual to have a prior process of charge separation so that electrons reside in one medium and holes reside in another. In this type of situation the overall recombination process consists of the interfacial charge transfer of an electron in the electron-transport medium to an electron-acceptor in the hole-transport medium. This is the type of process that we consider in the following discussion.

By analogy to the diffusion problem, one should distinguish between the jump (or single-particle) and small perturbation (or collective) lifetimes. The former, τ_J, is the survival time of the carriers and can be computed by averaging over the survival times of single particles in diffusion−recombination simulations.[50−52] We use the term *jump* for this quantity, just because, as we will see below, τ_J is the analogous quantity to the diffusion coefficient D_J. The latter, τ_n, is the time that appears in the continuity equation for a small perturbation of carriers and is of great importance in nanostructured solar cells.[53] τ_n is usually obtained by making a small step of excess carriers in the sample and then measuring the "time" for recovery.[54−56] Here we show that for an arbitrary recombination rate one needs two factors to link τ_n to τ_J: the classical thermodynamic factor, χ_n, and a recombination factor. χ_r, defined here for the first time by analogy to χ_n.

In principle, one could measure a large decay of an injected population of electrons, but as mentioned above, here we are concerned only with methods in which kinetic quantities can be associated with a stable local Fermi level in quasiequilibrium, which makes it necessary to use the small perturbation techniques as discussed elsewhere.[8,53] Let us consider the continuity equation in a spatially homogeneous Fermi level and in the absence of a generation term

$$\frac{dn}{dt} = -U(n) \tag{14}$$

where $U(n)$ is the total recombination rate per unit volume. Here, by recombination we mean the carrier transfer from the nanostructured electron-transport medium to the hole-transport material. $U(n)$ is, in general, a complicated function of the carrier density n. Therefore, solution of eq 14 does not yield an exponential decay. However, it is easy to show that a small perturbation of the population with respect to the average value, $\delta n \ll \bar{n}$, will decay exponentially with characteristic time of

$$\tau_n = \left(\frac{\partial U}{\partial n}\right)^{-1}_{\bar{n}} \tag{15}$$

τ_n is called the small perturbation lifetime and is experimentally accessible by many techniques, as widely used in the field of DSCs.[39]

Now, we introduce the *jump* or *single-particle* lifetime τ_J to differentiate it from the small perturbation lifetime, τ_n. As a definition, τ_J is the average of the survival time of the carriers

$$\tau_J = \langle t \rangle \tag{16}$$

Therefore, τ_J is the time it takes for the individual particles to recombine. So, to find τ_J, we have to monitor the recombination time of the individual particles. If we assume that the recombination is slow enough, like the case of DSCs, then it can be shown that the above equation can be written as

$$\tau_J = \frac{n}{U} \tag{17}$$

Equation 17 suggests that τ_J can be measured if one can determine the total charge participating in recombination as well as the total recombination flux at a given position of the Fermi level. A discussion of the conditions to perform such measurement lies beyond the scope of this paper. A rigorous but rather long derivation of eq 17 will be presented in a separate work. However, we note that this equation has a simple physical meaning. Assuming that there are N carriers in a system with volume V, $1/VU$ will be the average time that the first carrier recombines. Because we have N carriers, N/VU is the average time that a carrier survives before it recombines. Hence we come to $\tau_J = n/U$. This equivalence between eqs 16 and 17 has also been demonstrated by Monte Carlo simulation in ref 50 by comparing the lifetime obtained from the averaging of the survival times in steady-state simulations and the lifetime extracted from the decay of a population of carriers in the limit of small perturbations.

To find the relation between τ_J and τ_n, by analogy to eq 8 for the thermodynamic factor, we define the *recombination factor*, χ_r, as

$$\chi_r = \frac{U}{k_B T}\frac{\partial \mu}{\partial U} \tag{18}$$

χ_r is indicative of the recombination mechanism in the system. Identical to χ_n, if the recombination rate depends exponentially on μ/k_BT, one has $\chi_r = 1$. We use the term *linear recombination* in the case that $\chi_r = 1$. In the field of DSCs, "linear recombination" is used for situations in which the recombination rate is proportional to the carrier density in the conduction band, n_c. Because n_c is given by the Boltzmann statistics, it is easy to show that $\chi_r = 1$ is fulfilled in this case. Now, one can obtain the following general relation between lifetimes τ_J and τ_n

$$\tau_n = \frac{\chi_r}{\chi_n}\tau_J \tag{19}$$

For Boltzmann statistics and linear recombination, we have $\chi_n = 1$ and $\chi_r = 1$, respectively; therefore, there is no difference between the small perturbation and jump lifetime. However, these conditions are not usually met in the materials with distributions of localized states. As previously discussed, both site-saturation effects and interactions cause a variation of χ_n. In addition, the factor χ_r is usually larger than 1 for both inorganic and organic solar cells.[57−59]

Table 1. Comparison between the Quantities That Appear in the Continuity Equation (Chemical Diffusion Coefficient and Small Perturbation Lifetime) and the Ones That Are Related to the Individual Carriers (Jump Diffusion Coefficient and Lifetime)[a]

quantity	definition	multiple trapping expression	equality
chemical diffusion coefficient	$J_n = -D_n \frac{dn}{dx}$	$D_n = \left(1 + \frac{\partial n_L}{\partial n_c}\right)^{-1} D_0$	$D_n = \chi_n D_J$
jump diffusion coefficient	$D_J = \frac{1}{2dt}\left\langle \frac{1}{N}(\sum_i \Delta r_i)^2 \right\rangle$	$D_J = \left(1 + \frac{n_L}{n_c}\right)^{-1} D_0$	
small perturbation lifetime	$\tau_n = \left(\frac{\partial U}{\partial n}\right)^{-1}$	$\tau_n = \left(1 + \frac{\partial n_L}{\partial n_c}\right)\tau_f$	$\tau_n = \frac{\chi_r}{\chi_n}\tau_J$
jump lifetime	$\tau_J = \left(\frac{U}{n}\right)^{-1}$	$\tau_J = \left(1 + \frac{n_L}{n_c}\right)\tau_f^J$	
free electron lifetime		$\tau_f = \left(\frac{\partial U}{\partial n_c}\right)^{-1}$	$\tau_f = \chi_r \tau_f^J$
jump free electron lifetime		$\tau_f^J = \left(\frac{U}{n_c}\right)^{-1}$	

[a]In addition to the general definition for each quantity, the specific multiple trapping expressions are also shown in the Table. The last column shows the generally valid relationship between the parameters.

Table 1 shows the general definitions for the small perturbation and jump quantities. In this section, we tried to characterize the transport and recombination of the carriers in the system. However, we did not discuss the nature of transport and recombination. In the following section, we will adopt the MT model and specific types of charge transfer rate dependence on carrier density. Table 1 also shows the various quantities in the context of this specific model, as will be discussed in the next section.

3. MULTIPLE TRAPPING MODEL

The mechanism of electronic transport in a material is dictated by the nature of the electronic states: their energies and spatial locations and extensions. In general, three models can be considered to model the transport. In bulk crystalline materials, which can be characterized by well-defined band structures, the Boltzmann transport equation usually provides a good description of the electronic properties of the system.[60,61]

In the opposite limit, for instance, in semiconducting polymers and small molecules, because of the absence of the long-range crystalline order, the situation is different and electronic states are quite localized.[62] We will call these localized states *traps* because they effectively act as potential wells for electrons and holes in the material. In this case, as discussed in Introduction, the transport occurs by transition between the traps in the distribution (hopping transport), with a probability usually given by the Miller–Abrahams jump rate or by the Marcus transfer rate, depending on whether the conservation of energy in the charge-transfer event is realized by a single phonon or by solvent and vibronic reorganization effects. (For a comprehensive review, see ref 10.)

In inorganic nanocrystalline materials, for example, nanostructured metal oxides used in DSCs, one has both the extended states (conduction band states) and the localized states (trap states in the band gap). In this case, the classical MT model proved to be capable of describing the behavior of the transport coefficient observed in the experiment.[6,5] MT model includes two classes of carrier: (i) free or mobile carriers in the states above the mobility edge, E_0, also called conduction band carriers, and (ii) immobile or trapped carriers in the states below the mobility edge.

In the hopping transport model, for the exponential DOS[4,15] or for carriers situated deep enough energetically in an arbitrary DOS,[12] a particular level, called the transport energy, E_{tr}, determines the dominant hopping events. The transport energy essentially reduces the hopping transport to MT, with E_{tr} playing the role of the mobility edge E_0. (See also refs 63 and 6 and references therein). In the following, we use "C" (conduction) for both the mobility edge and the transport energy (hence E_C stands for either mobility edge, E_0, or transport energy, E_{tr}). We also use subscript "L" to denote localized states below the transport level.

3.1. Diffusion Coefficients. As discussed above, in the MT model, we need to distinguish between n_c, carrier density in the transport level, and n_L, carrier density in localized states, defined as

$$n_i = \int g_i(E) f(E - E_F)\, dE \tag{20}$$

where i stands for C or L. Therefore, for the total carrier density we can write

$$n = n_c + n_L \tag{21}$$

Both n_c and n_L are functions of Fermi level E_F. However, if we restrict our attention to the domain of potentials in which the Fermi level remains well below E_C, so that we avoid degeneracy effects, then the carrier density in transport level is well-described by Boltzmann statistics and therefore

$$n_c = N_c \exp\left(\frac{E_F - E_C}{k_B T}\right) \tag{22}$$

where N_c is the effective density of the transport level states.

When carrier transport is governed by activation to some type of transport level within a broad distribution of localized states, a great variation of the diffusion coefficient occurs as the Fermi level moves in the bandgap because the cost of promoting a carrier to the transport level is largely modified according to the occupation of the localized levels. Therefore, in disordered systems, diffusion coefficients and electron mobilities are density-dependent, with larger values found when the electron concentration is increased, either by illumination or by application of an external voltage. This situation is observed in both organic[64,65] and inorganic materials.[18,66,67]

dx.doi.org/10.1021/jp403232b | J. Phys. Chem. C 2013, 117, 16275–16289

On the basis of the *quasistatic approximation*, Bisquert and Vikhrenko showed that, in the context of the MT model, the chemical diffusion coefficient has the general form[7]

$$D_n = \left(1 + \frac{\partial n_L}{\partial n_c}\right)^{-1} D_0 \tag{23}$$

where D_0 is diffusion coefficient of the carriers in the transport level (in the absence of the trap states) and called the free-electron diffusion coefficient. The quasistatic approximation assumes that trapping and detrapping are fast processes, in comparison with the time scale in which the experimental measurement is carried out.[7] Note that in the MT model the diffusion coefficient consists of two parts. The first is the *trapping−detrapping factor*, $(1 + \partial n_L/\partial n_c)$ that relates to the equilibration of trapped and free electrons when the small perturbation of the density occurs. The second is the free-electron diffusion coefficient, D_0.

There is a simple but powerful derivation of eq 23. We note that the principle of detailed balance links the kinetic constants for trapping and detrapping to the equilibrium occupancies n_c and n_L. Therefore, electron-trapping kinetics can be readily described in terms of the electron densities in transport and trap states as[6]

$$\frac{D_J}{D_0} = \frac{n_c}{n_c + n_L} \tag{24}$$

Combining eq 24 and the relation $D_n = \chi_n D_J$, we arrive to eq 23. Equation 23 is very well-known in the field of DSCs and used routinely in the literature. In Section 3.4 we will return to the problem of MT transport. Using Monte Carlo simulation it will be shown that what one really obtains using the random-walk simulation, is D_J and not D_n, with D_n and D_J given by eq 23 and 24, respectively.

3.2. Recombination and Lifetime. Using the definition of small perturbation lifetime, eq 15, for τ_n, we find[53]

$$\tau_n = \left(1 + \frac{\partial n_L}{\partial n_c}\right)\tau_f \tag{25}$$

Similar to D_0 in eq 23, τ_f is called the free-electron lifetime and is defined as

$$\tau_f = \left(\frac{\partial U}{\partial n_c}\right)^{-1} \tag{26}$$

The partition of the lifetime in eq 25 indicates that the lifetime dependence on the Fermi level is governed by two different effects. The first, similar to the diffusion coefficient, eq 23, is the trapping−detrapping factor. The second is the charge-transfer rate across the interface and is described by τ_f.[53] The similar structure of eq 23 and eq 26, for the diffusion coefficient and lifetime, respectively, will be discussed in more detail in Section 3.5. However, we emphasize that unlike D_0, τ_f can be variable with Fermi level position if the electrons in the trap states contribute to the recombination (see later.)

For the jump lifetime, we can simply use eq 17 and write it in the form

$$\tau_J = \left(1 + \frac{n_L}{n_c}\right)\tau_f^J \tag{27}$$

where, by analogy to τ_f we have defined the *jump free electron lifetime*, τ_f^J, as

$$\tau_f^J \equiv \frac{U}{n_c} \tag{28}$$

Equation 27 is very suitable if we want to compare τ_J and τ_n and if we want to see the equivalence between the diffusion coefficient and the lifetime in the MT model, as we have shown in Table 1. The physical difference between the jump and small perturbation lifetime in the context of the MT model is also shown in Figure 1. As indicated in this Figure, τ_J is related to

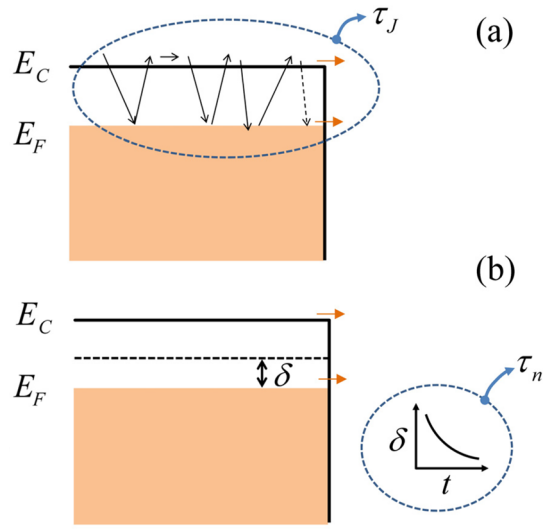

Figure 1. Difference between the jump and small perturbation lifetime. (a) τ_J is survival time of the carrier moving in a well-defined Fermi level. The carrier can recombine in the surface. Trapping−detrapping time and also the recombination rate at the surface determine the jump lifetime. (b) τ_n is related to the recovery time of the system after being perturbed by a small amount of δ. This small perturbation always decays exponentially, leading to a well-defined characteristic response time, that is, τ_n.

trapping−detrapping of the individual particles in the system. τ_n is the time for the recovery of the total equilibrium density, after perturbing the system by a small amount δ. A small perturbation guarantees an exponential decay of δ. Note that τ_n can only be defined for a quasiequilibrium decay process. τ_J can also be defined for equilibrium steady-state conditions.

Using the definition of the recombination factor χ_r in eq 18, we can find the following relation between the free and the jump free lifetime

$$\tau_f = \chi_r \tau_f^J \tag{29}$$

χ_r is determined by the recombination rate, U. When only the electrons in transport level participate in the recombination, we will have $U \propto n_c$. In this case, as previously discussed, $\chi_r = 1$ (linear recombination regime). Therefore τ_f and τ_f^J become equal and independent of the Fermi level. However, for example, in DSCs, electrons in the surface traps of the nanoparticles can directly recombine with the oxidized ions in the electrolyte, leading to a nonlinear dependence of U on n_c as[8]

$$U = k_r (n_c)^{\beta} \tag{30}$$

dx.doi.org/10.1021/jp403232b | J. Phys. Chem. C 2013, 117, 16275−16289

where β is the reaction order with respect to the carriers in the transport level and k_r is a constant. In the experiments, β is usually found in the range between 0.5 and 1. (In nanostructured quantum-dot-sensitized solar cells, β can be smaller than 0.5.) On the basis of this discussion, it is obvious that a more fundamental way to write the nonlinear recombination rate eq 30 is

$$U = U_c + U_L^{ss} \tag{31}$$

where U_c and U_L^{ss} are the recombination rate from the transport level and localized surface trap states, respectively. From the microscopic point of view, U_C and U_L^{ss} can be expressed as[68]

$$U_c = K(E_c)n_c \tag{32}$$

$$U_L^{ss} = \int K(E)g_L(E)f(E - E_F)\,dE \tag{33}$$

where $K(E)$ is the rate of charge transfer from the states with energy E. The exact form of $K(E)$ depends on the nature of the charge transfer. (In DSCs, usually Marcus rate of charge transfer is assumed in the literature.[26,51,68,69])

By comparing eq 30 with eq 31, it was recently shown that the reaction order can be expressed as[58]

$$\beta = 1 - \frac{\ln\left(1 + \frac{U_L^{ss}}{U_c}\right)}{\left|\ln\left(\frac{n_C}{N_C}\right)\right|} \tag{34}$$

which is always less than one when U_L^{ss} is nonzero. Equation 34 shows that the reaction order, in general, depends on the trap distribution and mechanism of the charge transfer and therefore is a function of the carrier concentration.[58]

Here we expressed the total recombination rate in two forms: eqs 30 and 31. These equations are appropriate for a system in which there are two kinds of electronic states, that is, extended states and localized states. (These different electronic states usually participate in the recombination with different time scales, and for this reason we separate their contributions in eq 31.) In the systems in which there are not any extended states (for example, conducting polymers), recombination rate is usually written in terms of the total density as n^α, where α is the reaction order with respect to the total density.[59] In general, although the number of carriers is obviously a function of the specific DOS, the main variable to compare several systems in a similar state is the Fermi level, which is experimentally given by the voltage. It should also be remarked that in systems with an extended state there is a simple correspondence between the free-carrier density and the voltage, established by eq 22. Therefore, in stochastic or random walk-simulation we often prepare a quasiequilibrium state by fixing a Fermi level, which experimentally is realized by applying a potentiostatic condition.

3.3. Multiple Trapping in the Exponential DOS. In the nanostructured metal oxides used in DSCs (and also in organic molecular crystals[70] and semicrystalline polymers[71]), the exponential DOS

$$g_L(E) = N_L \exp\left(\frac{E - E_C}{k_B T_0}\right) \tag{35}$$

seems to be able to reproduce the experimental observations. Here N_L is the total trap density and T_0 is a parameter with temperature units that determines the depth of the distribution below the transport level E_C. On the basis of the experimental evidence, at room temperature, $T_0/T \approx 2-5$.[16,72] The main features of MT transport model in the exponential DOS are amply described in recent papers,[9,48] and only a summary of the results is given here.

For the typical values of T_0, at low and intermediate Fermi level, $n_L \gg n_c$. Then

$$n \approx n_L \tag{36}$$

Under the zero-temperature approximation, one can find[7]

$$n_L = N_L \exp\left(\frac{E_F - E_C}{k_B T_0}\right) \tag{37}$$

Therefore, the thermodynamic factor in eq 8 is constant for exponential DOS and given by (for $T_0/T > 1$)[9]

$$\chi_n = \frac{T_0}{T} \tag{38}$$

Diffusion coefficient and lifetime can also be calculated using n_L in eq 37

$$D_n = \frac{T_0 N_c}{T N_L} \exp\left[(E_F - E_C)\left(\frac{1}{k_B T} - \frac{1}{k_B T_0}\right)\right] D_0 \tag{39}$$

$$\tau_n = \frac{T N_L}{T_0 N_c} \exp\left[(E_F - E_C)\left(\frac{1}{k_B T_0} - \frac{1}{k_B T}\right)\right] \tau_f \tag{40}$$

Using the relation between the jump and small perturbation quantities (Table 1) and χ_n in eq 38, one can also find D_J and τ_J in the MT model. (For τ_J we also need the recombination factor χ_r; see below.)

As previously discussed, τ_f in eq 40 is in general a function of the Fermi level. Let us consider the recombination rate of eq 30. With $\beta = 1$, it will be found, according to eq 18, that $\chi_r = 1$ (linear recombination). However, $\beta < 1$ is usually observed in the experiments. In the DSC literature, a constant reaction order β is commonly assumed (and observed experimentally) in the literature. *For constant* β it can be shown that by combining eqs 18, 22, and 30 one finds[58]

$$\chi_r = \frac{1}{\beta} \qquad [\text{constant } \beta] \tag{41}$$

In this case, for the relation between the jump and small perturbation lifetime in exponential DOS, we get[40,73,74]

$$\tau_J = \beta \frac{T_0}{T} \tau_n \qquad [\text{constant } \beta] \tag{42}$$

A constant β implies that χ_r is also constant. This constant χ_r is usually called the ideality factor. However, by exploring the response of the cell over a wide range of the incident illumination, experimental[57,75] and theoretical[58,59] studies have shown that χ_r and β are not constant. As explained above, β increases to unity by increasing the Fermi level. (See also ref 75.) In this case there is not a simple relation between β and χ_r. In ref 51, the β coefficient has been extracted from Monte Carlo simulation of DSCs, from both steady-state and charge extraction decay "experiments". The β coefficient is found to depend indeed on the trap distribution as well as on the relative alignment of energies between conduction band and the redox couple potential. In this respect, and in accordance to the predictions of eq 34, if the transport level is "close" to the redox

dx.doi.org/10.1021/jp403232b | J. Phys. Chem. C 2013, 117, 16275−16289

potential (Fermi level close to the transport level), then the β coefficient is found to approach one.

3.4. Multiple Trapping in a Gaussian DOS: Simulation Results. In disordered semiconducting polymers used, for example, in organic solar cells, the best agreement between the experiment and the theory has been obtained using the Gaussian DOS[20,76]

$$g_L = \frac{N_L}{\sqrt{2\pi\sigma^2}} \exp\left(-\frac{(E - E_{L0})^2}{2\sigma^2}\right) \tag{43}$$

where E_{L0} is the center of the distribution and σ is the width, on the order of 0.1 eV. To explore the MT transport, we should also specify the position of the transport level, E_C, above the Gaussian distribution of localized states (see Figure 2). The

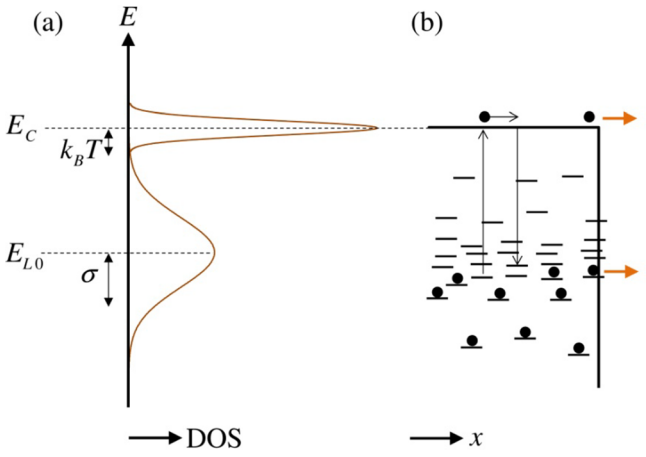

Figure 2. Multiple trapping transport and recombination in the Gaussian DOS. Trapping into the localized Gaussian DOS and then detrapping to the transport level (left) is essentially the same as the multiple trapping in the bi-Gaussian DOS (right), in which the upper Gaussian has a narrow wide on the order of thermal energy. For simulation of the recombination, we consider both the linear and nonlinear recombination. In the former, recombination occurs only when electrons are in the transport level. In the latter, recombination is also possible from trap states.

MT model consisting of the Gaussian DOS of eq 43 and a conduction band level at energy E_C has mainly been used in connection with light-emitting diodes.[77] It should also be noted that as shown in Figure 2 such model is in fact equivalent to the problem of the MT in a bi-Gaussian DOS,[64,76] in which the upper Gaussian, which plays the role of the transport level, has a narrow width on the order of k_BT.

MT (and also hopping) transport in the Gaussian DOS has been investigated in detail in ref 6. In general, as explained before, diffusion coefficient and mobility are increasing functions of the carrier concentration (or Fermi level). In the specific case of Gaussian DOS, unlike the exponential one, the thermodynamic factor χ_n is not constant. As we will see in the following, at low and high Fermi level, χ_n =1. However, at intermediate Fermi level, χ_n is (much) larger than unity (depending on the distance between E_C and E_{L0}). In this intermediate regime, the diffusion coefficient can be expressed analytically, as[6]

$$D_n = \frac{N_c}{N_L}\frac{\sqrt{2\pi\sigma^2}}{k_BT} \exp\left[\frac{(E_F - E_{L0})^2}{2\sigma^2} - \frac{E_C - E_F}{k_BT}\right] D_0 \tag{44}$$

Using eqs 23, 25, and 44, we can find a similar relation for the lifetime, as

$$\tau_n = \frac{N_L}{N_c}\frac{k_BT}{\sqrt{2\pi\sigma^2}} \exp\left[-\frac{(E_F - E_{L0})^2}{2\sigma^2} - \frac{E_F - E_C}{k_BT}\right] \tau_f \tag{45}$$

As previously mentioned, the thermodynamic factor in a Gaussian DOS is more structured than the exponential case. Therefore, the difference between the jump and the small perturbation quantities is not just a constant factor. For this reason, apart from its importance in the organic electronics, the Gaussian DOS is a good example to verify (i) the generalized Einstein relation, eq 7, (ii) the difference between D_n and D_J, eq 11, and (iii) the relationship between τ_n and τ_J, eq 19, using Monte Carlo simulation.

In traditional MT random-walk simulation, one only considers traps without explicit implementation of the transport level. However, the transport level is implicitly considered because the energy of the traps is defined with respect to a zero of energies (e.g., E_C in eq 44). These energies, as well as the spatial locations of the traps, are fixed before the simulation. Then, the simulation starts by putting the particles randomly on the traps and letting them to jump between traps. One can find the basic features of a Monte Carlo simulation based on the MT model in ref 23.

In contrast, and to make a quantitative comparison between the simulation results and the theoretical predictions, we consider here *explicitly* both the transport level and the trap states in the simulations: we run the simulations on a cubic lattice, with lattice spacing a. The lattice sites have energy E_C with probability of $N_C/(N_C + N_L)$; otherwise, their energy is taken from the Gaussian DOS eq 43.

At the beginning of our single-particle simulation,[26,78] lattice sites are occupied by the particles, according to the Fermi–Dirac distribution with an arbitrary Fermi level. Then, we put a test particle in an unoccupied site at random. At each simulation step, this particle is allowed to randomly jump to one of its empty nearest neighbors. Because we are simulating the MT transport, the time that the particle spends on the site with energy E_i is given by

$$t_i = \frac{X}{\nu_i} \tag{46}$$

where $\nu_i = \nu_0 \exp((E_i - E_C)/k_BT)$ is the thermal jump rate in which ν_0 is called the attempt-to-jump frequency. X for each jump is randomly generated with an exponential distribution with unit expectation value and unit variance. (See ref 46.) Finally, one can calculate the random walk diffusion coefficient using eq 13 with N = 1.

Because we also want to justify the validity of generalized Einstein relation by separate determination of its components, we also need to calculate the mobility from the Monte Carlo simulation. A detailed description of such a simulation can be found in refs 79–81. In summary, suppose that there is an electric field F in the x direction. This field causes the probability to jump to the left to be different from that to jump to the right, and thus each jump is biased. Here we assume that the ratio between these probabilities is given by the Boltzmann

dx.doi.org/10.1021/jp403232b | J. Phys. Chem. C 2013, 117, 16275–16289

factor, $\exp(qaF/k_BT)$.[81] Finally, after a fixed simulation time, t, the mobility can be calculated using the following relation

$$u^{sim} = \frac{\langle x \rangle}{Ft} \tag{47}$$

Simulation of the recombination process is a more subtle case. At the first step one should choose the model of charge transfer ($K(E)$ in eqs 32 and 33). We have recently used the Marcus rate for charge transfer as the recombination rate in our simulations[51,52]

$$K(E) = K^0 \exp\left(-\frac{(E - E_{F_0} - \lambda)^2}{4\lambda k_B T}\right) \tag{48}$$

where K^0, λ, and E_{F0} are the rate constant for charge transfer, the reorganization energy, and Fermi level before illumination (in DSCs, redox potential of the electrolyte), respectively. We also allow for different rate constants for transfer from the transport level (K_C^0) and trap states (K_L^0). At the next and more important step, one should adopt a method to convert the recombination rate to the Monte Carlo language. Here we have used the method of ref 52, in which the particle on the site with energy E_i recombines with probability $P = K(E_i)\, t_i$, where t_i is given by eq 46. For simulation of the linear recombination, we allowed the particle to recombine only when its energy was E_C. We used the periodic boundary condition in the simulations; therefore, there is not a real surface in the simulation, wherein recombination occurs. However, we can specify some sites on the lattice as *recombination centers*[50] so that the carrier can recombine only in these sites. (When the carrier reaches these sites, it recombines with the probability $P = K(E_i)t_i$.)

We used the following parameters in our simulations: T = 300 K, ν_0 = 2 THz, E_C = 0, E_{L0} = −0.25 eV, σ = 0.08 eV, qaF = 0.4σ, N_L/N_c = 0.25, K_C^0 = 1.76 GHz, K_L^0 = 1.76 MHz, E_{F0} = −0.8 eV, and λ = 0.6 eV. Also, a = 1 nm was used for the lattice spacing. This implies that in eq 23 $D_0 = \nu_0 a^2/6 = 0.33 \times 10^{-2}$ cm^2 s^{-1}. Note that the values of a can be rescaled to fit specific data without modifying the general behavior of the model. For the simulation of diffusion, ν_0 can be viewed as an adjustable parameter that controls the time scale of the simulation. However, as we will see in Section 3.5, this parameter, together with the values of K_C^0 and K_L^0, has a very important role in the simulation of recombination. The values of other parameters are realistic, as can be found in literature.

Figure 3 shows the thermodynamic factor for the Gaussian DOS. As can be seen, unlike the case of exponential DOS, this factor is a function of the Fermi level. To obtain the thermodynamic factor from the simulation, for each Fermi level we numerically calculate the quantity

$$\chi_n^{sim} = \frac{\langle n \rangle}{k_B T}\left(\frac{\partial \langle n \rangle}{\partial E_F}\right)^{-1} \tag{49}$$

where $\langle n \rangle$ is the average of the density of occupied lattice sites. In the organic polymers, the upper Gaussian usually does not exist in the material. In this case, as indicated in the Figure 3, thermodynamic factor will grow unlimitedly because of the exhaustion of available empty sites, but in the presence of a transport level, at high E_F, the thermodynamic factor approaches unity.

Results for the diffusion coefficient are shown in Figure 4. First of all, it can be observed that the diffusion coefficient obtained in the simulation, D^{sim}, is in excellent agreement with the MT prediction D_J of eq 24. This confirms the statement that the random walk diffusion coefficient is different from the one that appears in Fick's law. To check the validity of the relation $D_n = \chi_n D_J$, we also compute the product $\chi_n^{sim} D^{sim}$. As can be seen in Figure 4, this quantity also is in good agreement with the MT prediction, D_n, of eq 23.

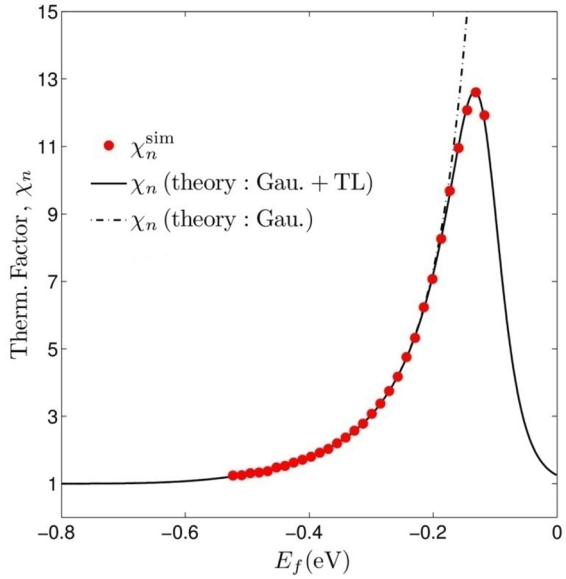

Figure 3. Thermodynamic factor versus Fermi level for the energy-level alignment of Figure 2. The points are the Monte Carlo simulation results, computed using eq 49, and the solid line is the theoretical value for thermodynamic factor calculated with eq 8. Also shown (dashed line) is the thermodynamic factor for the Gaussian distribution, without the transport level (TL). In this case, thermodynamic factor diverges at high Fermi level. See the text for the parameters used in the calculation.

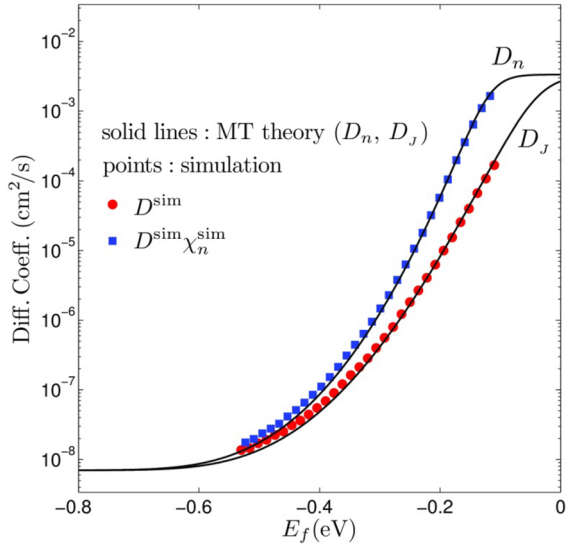

Figure 4. Diffusion coefficient versus Fermi level for multiple trapping in the Gaussian DOS. The lines show the theoretical predictions for D_n and D_J, calculated with eqs 23 and 24, respectively. The filled circles (D^{sim}) show the random walk diffusion coefficient obtained in the simulation. As can be seen, D^{sim} coincides with the jump coefficient, D_J. Filled squares show the quantity $D^{sim}\chi_n^{sim}$. The results are in agreement with the chemical diffusion coefficient D_n.

dx.doi.org/10.1021/jp403232b | J. Phys. Chem. C 2013, 117, 16275−16289

As discussed in Section 2.2, there are two statements for the generalized Einstein relation, eqs 7 and 12. Both statements were verified in the simulations. We first computed the mobility u^{sim} from the simulation. Then, using the simulation result for diffusion coefficient in Figure 4, the ratio D^{sim}/u^{sim} was calculated. The result of such calculation is shown in Figure 5. As previously mentioned, the simulations were done at 300

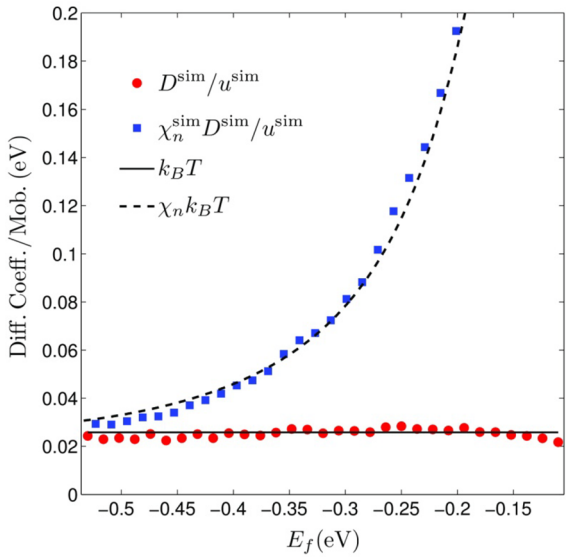

Figure 5. Einstein relation for multiple trapping in the Gaussian DOS. The filled circles show the Monte Carlo simulation results. For each point we have done two separate simulations, one without the electric field to calculate the diffusion coefficient D^{sim} and another one with electric field to compute the mobility u^{sim}. As can be seen, results of the simulation are in good agreement with prediction $D_J/u_n = k_BT/q$ = 0.258 eV, eq 12. The dashed line and the filled squares show the other statement of the generalized Einstein relation, that is, eq 7. Note that *both* sets of data justify the generalized relationship.

K. Thus, based on eq 12, we expect that D^{sim}/u^{sim} = 0.258 eV for all Fermi levels. This prediction is indeed met, as plotted in Figure 5 (filled points). Using $\chi_n^{sim} D^{sim}/u^{sim}$, one can also test eq 7 (squares in Figure 5). Note that *both curves* in Figure 5 show the validity of the generalized Einstein relation, at least for the temperature and strength of the electric field studied here. Very recently, simulations employing explicitly the hopping model have also proved this validity.[82] As discussed in Introduction, recently Wetzelaer et al. argued that under the equilibrium conditions the *classical* Einstein relation eq 9 is always satisfied.[37] Their conclusion was based on the assumption that the generalized Einstein relation is linked to the ideality factor (here, recombination factor) appearing in the diode equation. However, based on the theory in Section 2.2, we saw that the generalized Einstein is expressed in terms of the thermodynamic factor and not the recombination factor. (See also ref 83.) In fact, the results of the calculations in Figure 5 show that, even at equilibrium, if the thermodynamic factor deviates from unity (when the distribution of the carriers is not given by Boltzmann statistics), then the classical Einstein relation will not hold, as it is well known in the literature of semiconductors.

To complete the discussion, we have also compared the lifetimes obtained from the simulations with theoretical predictions of eq 25 and eq 27. Results are shown in Figure 6 for both linear and nonlinear recombination. As we expect,

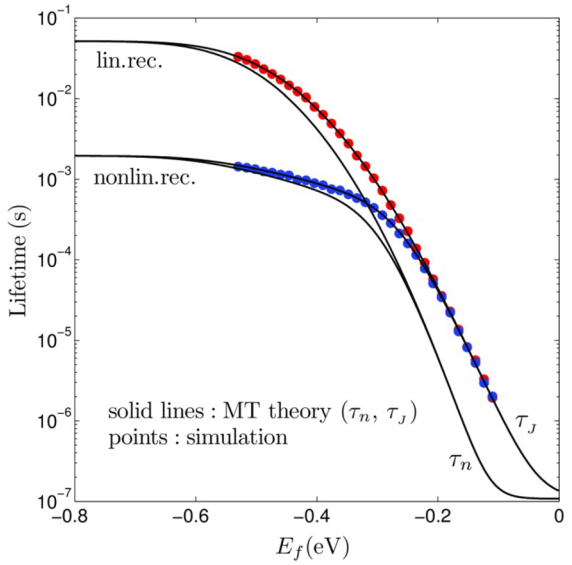

Figure 6. Lifetime versus Fermi level for recombination in the Gaussian DOS. The points show the lifetime obtained from the simulation. As can be seen, for both the linear and nonlinear recombination, random walk simulation lifetime coincides with the jump lifetime, τ_J, and not with the small perturbation lifetime, τ_n. In nonlinear recombination, at low Fermi level, lifetime is lower than the linear one because recombination is also possible from the localized states. At higher Fermi level, linear and nonlinear recombination become equal because at these Fermi levels the main contribution to the recombination is due to the recombination from the transport level.

random walk lifetime is equal to τ_J and not τ_n. To see the difference between the recombination rate in linear and nonlinear recombination, one can compute the recombination rate as

$$U^{sim} = \frac{\langle n \rangle}{\tau^{sim}} \tag{50}$$

Using this rate, the recombination factor can also be computed from the simulation. The results for the recombination rate and the recombination factor are shown in Figure 7. In the nonlinear recombination, at a fixed Fermi level, recombination rate is larger than the linear one. Also, as can be seen in this Figure, χ_r is not constant. For exponential DOS, also a similar curve is obtained.[58,84]

3.5. Reaction-Limited versus Diffusion-Limited Recombination. In the MT model, there are opposite dependences of D_n and τ_n with respect to the Fermi level (suppose that τ_f is independent of the Fermi level), as can be seen from the general relation eqs 23 and 25 for diffusion coefficient and lifetime. Strictly speaking, the so-called trapping−detrapping term, $(1 + \partial n_L/\partial n_c)$, affects D_n and τ_n in the opposite directions. To explain this opposite behavior, some authors suggested that the recombination process is *diffusion-limited* in DSCs: if the carrier transport becomes faster when the Fermi level is increased, then the probability for an electron to find a target to recombine is larger so that the electron lifetime is reduced.[85−88] This picture is also known as *transport-limited recombination*. This problem has already been well-discussed by Bisquert and Vikhrenko[7] to interpret the experimental result of Kopidakis et al.[85] for time constants in DSCs. They[7] explained that in DSCs, where MT model has

dx.doi.org/10.1021/jp403232b | J. Phys. Chem. C 2013, 117, 16275−16289

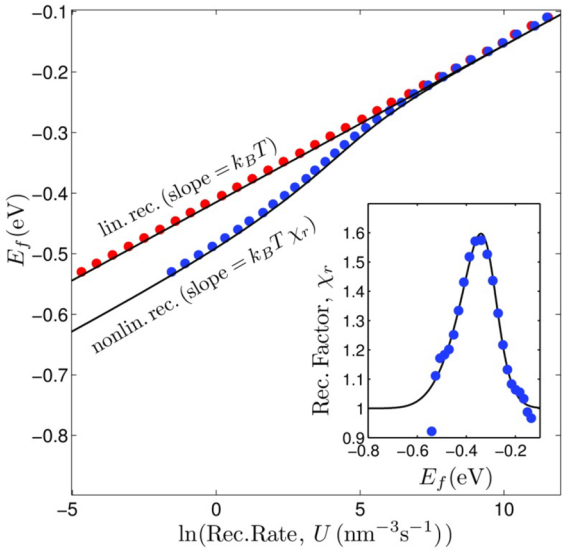

Figure 7. Fermi level versus recombination rate. The points show the simulation results, computed using eq 50. Solid lines are the theoretical value, calculated with eqs 31−33 and 48. The slope of these curves gives the quantity $k_BT\chi_r$. For linear recombination, χ_r =1. In the nonlinear case, both the theoretical value and the simulation result for χ_r are shown in the inset.

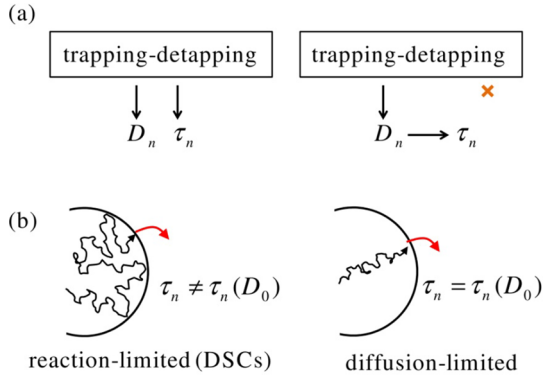

Figure 8. Reaction-limited versus diffusion-limited recombination. (a) Right: In the diffusion-limited recombination, trapping−detrapping factor in the lifetime relation comes from the diffusion coefficient. As we discussed in the text, this is not the case that takes place in the systems as DSCs. Left: On the basis of the discussion in the text, in quasistatic approximation, trapping−detrapping factor can independently be obtained for both the diffusion coefficient and the lifetime. (b) Left: Recombination events usually takes place in the interface that separates the electron-conducting phase from the hole-conducting one. As a result, for recombination, charge carriers should reach the surface. When the recombination rate is very small, charge carriers meet the interface numerous times. In this case. only the surface-to-volume ratio is important and recombination is reaction-limited. Right: in contrast, when the recombination is a fast process, charge carriers recombine upon reaching the surface. Recombination in this case is diffusion-limited, and transport speed, given by free electron diffusion coefficient, determines the lifetime.

been a successful model, the recombination is reaction-*limited*. We discuss this problem in this section.

Note that for derivation of the lifetime definition, eq 15, we wrote the continuity equation for a homogeneous Fermi level; therefore, we could ignore the diffusion term. As a result, the trapping−detrapping term has entered into the lifetime expression, eq 25, irrespective of the form of the diffusion coefficient. In other words, as shown schematically in Figure 8a, the traps *directly* affect the time constant of the recombination. In addition, when τ_f is a function of Fermi level (nonlinear recombination), the change of the lifetime with Fermi level is not just the inverse of the change in the diffusion coefficient. This shows that $\tau_n \propto 1/D_n$ in the linear recombination is merely due to the trapping−detrapping and not because of the diffusion-limited recombination.

It may be argued that diffusion coefficient can influence the lifetime via D_0: with a larger D_0, carriers will move with a higher *speed* and therefore can find a target for recombination more rapidly. This issue has been clearly shown in Figure 8b. We note that in DSCs, for a nanoparticle of radius of 10 nm, the time for the carriers to reach the surface is much shorter than the recombination time.[7] Therefore, carriers may meet the surface numerous times before they actually recombine. As a consequence, it is merely the surface-to-volume ratio that plays an important role in the recombination rate and not the speed by which carriers reach to the surface. This is just the reaction-limited regime. In contrast, in the diffusion-limited regime, the carriers most likely recombine upon their first encounter with the surface; therefore, the transport speed will be the main determining factor in the lifetime. (See refs 89 and 90 and references therein.)

To justify this subject, we did simulations at a fixed Fermi level and with different values of D_0. (See also ref 88.) As previously explained, $D_0 = \nu_0 a^2/6$. Therefore, we can simply change the jump frequency ν_0 to obtain an arbitrary D_0. Results of such simulation, for the linear recombination, are shown in Figure 9. As can be seen in this Figure, at high jump frequencies

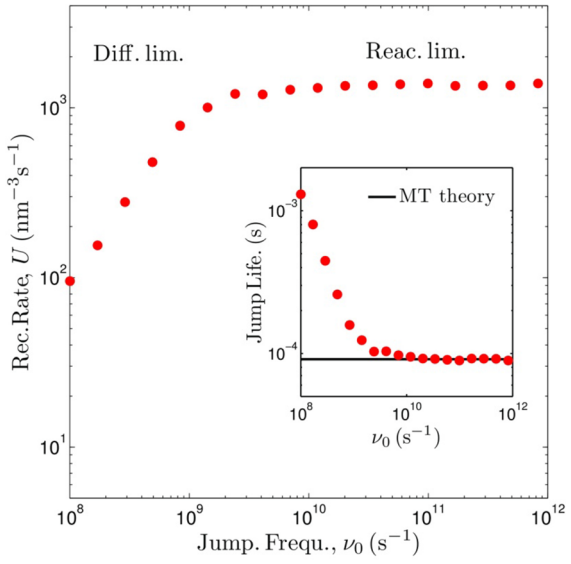

Figure 9. Recombination rate, U, versus the jump frequency, ν_0. Simulation was done at fixed Fermi level E_F = −0.22 eV, and eq 50 was used for calculation of the recombination rate. As can be seen, depending on the ν_0, recombination can be diffusion-limited or reaction-limited. Physical difference between these two regimes has been shown in Figure 8b. Inset: jump lifetime versus ν_0. Note that results of the simulation (filled circles) coincide with MT prediction, eq 27 (solid line), only in the reaction-limited region.

(small diffusion times) the total recombination rate, U, is independent of ν_0 (according to the Figure 8b, left), but in contrast, at low ν_0, U varies with ν_0 (as suggested by Figure 8b, right). Therefore, there is a clear transition between the diffusion-limited and reaction-limited regime, as indicated in

dx.doi.org/10.1021/jp403232b | J. Phys. Chem. C 2013, 117, 16275−16289

Figure 9. Note that in the diffusion-limited regime one cannot simply write the continuity equation as eq 14, and hence MT expression for lifetime eq 27 is not correct in this regime. To emphasize this problem, we have also shown lifetime versus jump frequency in Figure 9 and compared the results of the simulation with the prediction of the MT model, eq 27. Note that only in the reaction-limited regime do results of the simulation coincide with MT prediction. We also noticed (not shown here) that in the diffusion-limited regime, the value $\tau \times \nu_0$ is constant versus ν_0. This means that in this regime $\tau \propto 1/D_0$. To conclude, note that by changing the charge-transfer rate $K(E)$ (while keeping ν_0 fixed) one can also observe the transition from the reaction-limited to the diffusion-limited regime.

4. CONCLUSIONS

We have established a classification of different quantities that characterize carrier transport and recombination in the energetically disordered materials. It was found to be necessary to distinguish carefully between two different forms of the diffusion coefficient and lifetime: (i) small perturbation (or collective) quantities, D_n and τ_n, and (ii) jump (or single-particle) quantities, D_J and τ_J. The former are the parameters that appear in the continuity equation for a small perturbation of the charge carriers and therefore can easily be measured in the experiment, and the latter are those that are related to the behavior of the individual carriers, easily accessible in the simulations. The connections between these two forms are given by the thermodynamic factor χ_n and recombination factor χ_r. In the case of the MT transport model, we also emphasized several analogies between the diffusion problem and the lifetime one. However, we discussed that despite these similarities, in nanostructured photovoltaic systems such as DSCs, diffusion coefficient and lifetime are independent of each other and therefore recombination is a reaction-limited process. We tested all of the parameters defined in the text by the powerful tool of Monte Carlo simulation. We also showed that the validity of the generalized Einstein relation in the case of non-Boltzmann distribution of the carriers can be easily demonstrated in the simulation.

AUTHOR INFORMATION

Notes

The authors declare no competing financial interest.

Biographies

Mehdi Ansari-Rad received his B.S. (physics, 2007) and M.S. (solid state physics, 2009) from University of Tehran. Currently, he is a fourth year Ph.D. student in solid state physics at University of Tehran. His thesis work is focused on study of charge transport and recombination in dye-sensitized solar cells.

Juan A. Anta is Professor of Physical Chemistry at the University Pablo de Olavide, Seville. He received his Ph.D. in physical chemistry from the University Complutense de Madrid in 1997 and was a postdoctoral fellow in the Department of Theoretical Chemistry of the University of Oxford, where he worked on numerical simulation of quantum fluids. From mid-1999 to mid-2000 he was a postdoc at the Department of Chemistry of the Imperial College, London. His research interest focuses on solar cell modeling and characterization, computer simulation, and nanostructured solar cells.

Juan Bisquert is a Professor of Applied Physics at Universitat Jaume I de Castelló. He conducts experimental and theoretical research on nanoscale devices for production and storage of clean energies. His main topics of interest are dye- and quantum-dot-sensitized solar cells, organic solar cells, and solar fuel production. He has developed the application of measurement techniques and physical modeling that relate the device operation with the elementary steps that take place at the nanoscale dimension: charge transfer, carrier transport, chemical reaction, and so on, especially in the field of impedance spectroscopy as well as general device models.

ACKNOWLEDGMENTS

We acknowledge support of Generalitat Valenciana, project ISIC/2012/008. J.A.A. thanks Abengoa Research for support under Framework Collaboration.

REFERENCES

(1) Hagfeldt, A.; Boschloo, G.; Sun, L.; Kloo, L.; Pettersson, H. Dye-Sensitized Solar Cells. *Chem. Rev.* **2010**, *110*, 6595−6663.
(2) Gunes, S.; Neugebauer, H.; Sariciftci, N. S. Conjugated Polymer-Based Organic Solar Cells. *Chem. Rev.* **2007**, *107*, 1324−1338.

(3) *Organic Light-Emitting Devices: A Survey*; Shinar, J., Ed.; Springer: New York, 2004.
(4) *Charge Transport in Disordered Solids with Applications to Electronics*; Baranovskii, S. D., Ed.; Wiley: Weinheim, Germany, 2006.
(5) Anta, J. A. Electron Transport in Nanostructured Metal-Oxide Semiconductors. *Curr. Opin. Colloid Interface Sci.* **2012**, *17*, 124−131.
(6) Bisquert, J. Interpretation of Electron Diffusion Coefficient in Organic and Inorganic Semiconductors with Broad Distributions of States. *Phys. Chem. Chem. Phys.* **2008**, *10*, 3175−3194.
(7) Bisquert, J.; Vikhrenko, V. S. Interpretation of the Time Constants Measured by Kinetic Techniques in Nanostructured Semiconductor Electrodes and Dye-Sensitized Solar Cells. *J. Phys. Chem. B* **2004**, *108*, 2313−2322.
(8) Bisquert, J.; Mora-Sero, I. Simulation of Steady-State Characteristics of Dye-Sensitized Solar Cells and the Interpretation of the Diffusion Length. *J. Phys. Chem. Lett.* **2010**, *1*, 450−456.
(9) Bisquert, J. Chemical Diffusion Coefficient of Electrons in Nanostructured Semiconductor Electrodes and Dye-Sensitized Solar Cells. *J. Phys. Chem. B* **2004**, *108*, 2323−2332.
(10) Tessler, N.; Preezant, Y.; Rappaport, N.; Roichman, Y. Charge Transport in Disordered Organic Materials and Its Relevance to Thin-Film Devices: A Tutorial Review. *Adv. Mater.* **2009**, *21*, 2741−2761.
(11) Grünewald, M.; Thomas, P. A Hopping Model for Activated Charge Transport in Amorphous Silicon. *Phys. Status Solidi B* **1979**, *94*, 125−133.
(12) Baranovskii, S. D.; Faber, T.; Hensel, F.; Thomas, P. The Applicability of the Transport-Energy Concept to Various Disordered Materials. *J. Phys.: Condens. Matter* **1997**, *9*, 2699.
(13) Arkhipov, V. I.; Emelianova, E. V.; Adriaenssens, G. J. Effective Transport Energy versus the Energy of Most Probable Jumps in Disordered Hopping Systems. *Phys. Rev. B* **2001**, *64*, 125125.
(14) Baranovskii, S. D.; Cordes, H.; Hensel, F.; Leising, G. Charge-Carrier Transport in Disordered Organic Solids. *Phys. Rev. B* **2000**, *62*, 7934−7938.
(15) Bisquert, J. Hopping Transport of Electrons in Dye-Sensitized Solar Cells. *J. Phys. Chem. C* **2007**, *111*, 17163−17168.
(16) Bisquert, J.; Fabregat-Santiago, F.; Mora-Sero, I.; Garcia-Belmonte, G.; Barea, E. M.; Palomares, E. A Review of Recent Results on Electrochemical Determination of the Density of Electronic States of Nanostructured Metal-Oxide Semiconductors and Organic Hole Conductors. . *Inorg. Chim. Acta* **2008**, *361*, 684−698.
(17) Berger, T.; Anta, J. A.; Morales-Flórez, V. Electrons in the Band Gap: Spectroscopic Characterization of Anatase TiO_2 Nanocrystal Electrodes Under Fermi Level Control. *J. Phys. Chem. C* **2012**, *116*, 11444−11455.
(18) Guillen, E.; Peter, L. M.; Anta, J. A. Electron Transport and Recombination in ZnO-Based Dye-Sensitized Solar Cells. *J. Phys. Chem. C* **2011**, *115*, 22622−22632.
(19) Quintana, M.; Edvinsson, M.; Hagfeldt, T.; Boschloo, A. Comparison of Dye-Sensitized ZnO and TiO_2 Solar Cells: Studies of Charge Transport and Carrier Lifetime. *J. Phys. Chem. C* **2007**, *111*, 1035−1041.
(20) Oelerich, J. O.; Huemmer, D.; Baranovskii, S. D. How to Find Out the Density of States in Disordered Organic Semiconductors. *Phys. Rev. Lett.* **2012**, *108*, 226403.
(21) Bassler, H. Charge Transport in Disordered Organic Photoconductors a Monte Carlo Simulation Study. *Phys. Status Solidi B* **1993**, *175*, 15−56.
(22) Nelson, J.; Chandler, R. E. Random Walk Models of Charge Transfer and Transport in Dye Sensitized Systems. *Coord. Chem. Rev.* **2004**, *248*, 1181−1194.
(23) Anta, J. A. Random Walk Numerical Simulation for Solar Cell Applications. *Energy Environ. Sci.* **2009**, *2*, 387−392.
(24) Benkstein, K. D.; Kopidakis, N.; van de Lagemaat, J.; Frank, A. J. Influence of the Percolation Network Geometry on Electron Transport in Dye-Sensitized Titanium Dioxide Solar Cells. *J. Phys. Chem. B* **2003**, *107*, 7759−7767.
(25) Anta, J. A.; Morales-Florez, V. Combined Effect of Energetic and Spatial Disorder on the Trap-Limited Electron Diffusion Coefficient of Metal-Oxide Nanostructures. *J. Phys. Chem. C* **2008**, *112*, 10287−10293.
(26) Ansari-Rad, M.; Arzi, E.; Abdi, Y. Monte Carlo Random Walk Simulation of Electron Transport in Dye-Sensitized Nanocrystalline Solar Cells: Influence of Morphology and Trap Distribution. *J. Phys. Chem. C* **2012**, *116*, 3212−3218.
(27) Gonzalez-Vazquez, J. P.; Morales-Flórez, V.; Anta, J. A. How Important is Working with an Ordered Electrode to Improve the Charge Collection Efficiency in Nanostructured Solar Cells? *J. Phys. Chem. Lett.* **2012**, *3*, 386−393.
(28) Butcher, P. N. On the Definition of Energy Dependent Mobility and Diffusivity. *J. Phys. C: Solid State Phys.* **1972**, *5*, 3164−3167.
(29) Landsberg, P. T. Einstein and Statistical Thermodynamics. III. The Diffusion-Mobility Relation in Semiconductors. *Eur. J. Phys.* **1981**, *2*, 213−219.
(30) Ando, T.; Fowler, A. B.; Stern, F. Electronic Properties of Two-Dimensional Systems. *Rev. Mod. Phys.* **1982**, *54*, 437−672.
(31) Lee, P. A. Density of States and Screening near the Mobility Edge. *Phys. Rev. B* **1982**, *26*, 5882−5885.
(32) Marshak, A. H. Modeling Semiconductor Devices with Position-Dependent Material Parameters. *IEEE Trans. Electron Devices* **1989**, *36*, 1764−1772.
(33) Richert, R.; Pautmeier, L.; Bassler, H. Diffusion and Drift of Charge Carriers in a Random Potential: Deviation from Einstein's Law. *Phys. Rev. Lett.* **1989**, *63*, 547.
(34) Baranovskii, S. D.; Faber, T.; Hensel, F.; Thomas, P. On the Einstein Relation for Hopping Electrons. *Phys. Status Solidi B* **1998**, *205*, 87−90.
(35) Ritter, D.; Zeldov, E.; Weiser, K. Ambipolar Transport in Amorphous Semiconductors in the Lifetime and Relaxation-Time Regimes Investigated by the Steady-State Photocarrier Grating Technique. *Phys. Rev. B* **1988**, *38*, 8296−8304.
(36) Roichman, Y.; Tessler, N. Generalized Einstein Relation for Disordered Semiconductors- Implications for Device Performance. *Appl. Phys. Lett.* **2002**, *80*, 1948.
(37) Wetzelaer, G. A. H.; Koster, L. J. A.; Blom, P. M. Validity of the Einstein Relation in Disordered Organic Semiconductors. *Phys. Rev. Lett.* **2011**, *107*, 066605.
(38) Würfel, P. *Physics of Solar Cells: From Principles to New Concepts*; Wiley-VCH: Weinheim, Germany, 2005.
(39) Li, L.; Chang, Y.; Wu, H.; Diau, E. W. Characterisation of Electron Transport and Charge Recombination Using Temporally Resolved and Frequency-Domain Techniques for Dye-Sensitised Solar Cells. *Int. Rev. Phys. Chem.* **2012**, *31*, 420−467.
(40) Barnes, P. R. F.; Miettunen, K.; Li, X.; Anderson, A. Y.; Bessho, T.; Gratzel, M.; ORegan, B. C. Interpretation of Optoelectronic Transient and Charge Extraction Measurements in Dye-Sensitized Solar Cells. *Adv. Mater.* **2013**, *25*, 1881−1922.
(41) Callen, H. B. *Thermodynamics and an Introduction to Thermostatistics*, 2nd ed.; Wiley: New York, 1985.
(42) Teitel, S. D. S.; Shapir, Y.; Chimowitz, E. H. Monte Carlo Simulation of Fickian Diffusion in the Critical Region. *J. Chem. Phys.* **2007**, *116*, 3012−3017.
(43) Van der Ven, A.; Ceder, G.; Asta, M.; Tepesch, P. D. First-Principles Theory of Ionic Diffusion with Nondilute Carriers. *Phys. Rev. B* **2001**, *64*, 184307.
(44) Atkins, P. W. *Physical Chemistry*, 6th ed.; Oxford University Press: New York, 1998.
(45) Taylor, R.; Krishna, R. *Multicomponent Mass Transfer*; John Wiley & Sons: New York, 1993.
(46) Ala-Nissilay, T.; Ferrando, R.; Yingz, S. C. Collective and Single Particle Diffusion on Surfaces. *Adv. Phys.* **2002**, *51*, 949−1078.
(47) Gomer, R. Diffusion of Adsorbates on Metal Surfaces. *Rep. Prog. Phys.* **1990**, *53*, 917−1002.
(48) Bisquert, J. Physical Electrochemistry of Nanostructured Devices. *Phys. Chem. Chem. Phys.* **2008**, *10*, 49−72.
(49) van de Lagemaat, J.; Kopidakis, N.; Neale, N. R.; Frank, A. J. Effect of Nonideal Statistics on Electron Diffusion in Sensitized Nanocrystalline TiO_2. *Phys. Rev. B* **2005**, *71*, 035304.

(50) Gonzalez-Vazquez, J. P.; Anta, J. A.; Bisquert, J. Determination of the Electron Diffusion Length in Dye-Sensitized Solar Cells by Random Walk Simulation: Compensation Effects and Voltage Dependence. *J. Phys. Chem. C* **2010**, *114*, 8552−8558.
(51) Gonzalez-Vazquez, J. P.; Oskam, G.; Anta, J. A. A. Origin of Nonlinear Recombination in Dye-Sensitized Solar Cells: Interplay Between Charge Transport and Charge Transfer. *J. Phys. Chem. C* **2012**, *116*, 22687−22697.
(52) Ansari-Rad, M.; Arzi, E.; Abdi, Y. Simulation of Non-Linear Recombination of Charge Carriers in Sensitized Nanocrystalline Solar Cells. *J. Appl. Phys.* **2012**, *112*, 074319.
(53) Bisquert, J.; Fabregat-Santiago, F.; Mora-Sero, I.; Garcia-Belmonte, G.; Gimenez, S. Electron Lifetime in Dye-Sensitized Solar Cells: Theory and Interpretation of Measurements. *J. Phys. Chem. C* **2009**, *113*, 17278−17290.
(54) Schlichthorl, G.; Huang, S. Y.; Sprague, J.; Frank, A. J. Band Edge Movement and Recombination Kinetics in Dye-Sensitized Nanocrystalline TiO_2 Solar Cells: A Study by Intensity Modulated Photovoltage Spectroscopy. *J. Phys. Chem. B* **1997**, *101*, 8141−8155.
(55) Nakade, S.; Saito, Y.; Kubo, W.; Kanzaki, T.; Kitamura, T.; Wada, Y.; Yanagida, S. Laser-Induced Photovoltage Transient Studies on Nanoporous TiO_2 Electrodes. *J. Phys. Chem. B* **2004**, *108*, 1628−1633.
(56) Fabregat-Santiago, F.; Bisquert, J.; Chen, P.; Wang, M.; Zakeeruddin, S. M.; Gratzel, M. Electron Transport and Recombination in Solid-State Dye Solar Cell with Spiro-OMeTAD as Hole Conductor. *J. Am. Chem. Soc.* **2009**, *131*, 558−562.
(57) Salvador, P.; Hidalgo, M. G.; Zaban, A.; Bisquert, J. Illumination Intensity Dependence of the Photovoltage in Nanostructured TiO_2 Dye-Sensitized Solar Cells. *J. Phys. Chem. B* **2005**, *109*, 15915−15926.
(58) Ansari-Rad, M.; Arzi, E.; Abdi, Y. Reaction Order and Ideality Factor in Dye-Sensitized Nanocrystalline Solar Cells: A Theoretical Investigation. *J. Phys. Chem. C* **2012**, *116*, 10867−10872.
(59) Kirchartz, T.; Nelson, J. Meaning of Reaction Orders in Polymer:Fullerene Solar Cells. *Phys. Rev. B* **2012**, *86*, 165201.
(60) Jacoboni, C.; Reggiani, L. The Monte Carlo Method for the Solution of Charge Transport in Semiconductors with Applications to Covalent Materials. *Rev. Mod. Phys.* **1983**, *55*, 645−705.
(61) Jacoboni, C. *Theory of Electron Transport in Semiconductors*; Springer: Berlin Heidelberg, 2010.
(62) Mott, N. F. Conduction in Non-Crystalline Materials. *Philos. Mag.* **1969**, *19*, 835−852.
(63) Gonzalez-Vazquez, J. P.; Anta, J. A.; Bisquert, J. Random Walk Numerical Simulation for Hopping Transport at Finite Carrier Concentrations: Diffusion Coefficient and Transport Energy Concept. *Phys. Chem. Chem. Phys.* **2009**, *11*, 10359−10367.
(64) Coehoorn, R.; Pasveer, W. F.; Bobbert, P. A.; Michels, M. A. J. Charge-Carrier Concentration Dependence of The Hopping Mobility in Organic Materials with Gaussian Disorder. *Phys. Rev. B* **2005**, *72*, 155206.
(65) Pasveer, W. F.; Cottaar, J.; Tanase, C.; Coehoorn, R.; Bobbert, P. A.; Blom, P. W. M.; de Leeuw, D. M.; Michels, M. A. J. Unified Description of Charge-Carrier Mobilities in Disordered Semiconducting Polymers. *Phys. Rev. Lett.* **2005**, *94*, 206601.
(66) Tiwana, P.; Docampo, P.; Johnston, M. B.; Snaith, H. J.; Herz, L. Electron Mobility and Injection Dynamics in Mesoporous ZnO, SnO_2, and TiO_2 Films used in Dye-Sensitized Solar Cells. *ACS Nano* **2011**, *5*, 5158−5166.
(67) Gonzalez-Pedro, V.; Xu, X.; Mora-Sero, I.; Bisquert, J. Modeling High-Efficiency Quantum Dot Sensitized Solar Sells. *ACS Nano* **2010**, *4*, 5783−5790.
(68) Bisquert, J.; Zaban, A.; Greenshtein, M.; Mora-Sero, I. Determination of Rate Constants for Charge Transfer and the Distribution of Semiconductor and Electrolyte Electronic Energy Levels in Dye-Sensitized Solar Cells by Open-Circuit Photovoltage Decay Method. *J. Am. Chem. Soc.* **2004**, *126*, 13550−13559.
(69) Ondersma, J. W.; Hamann, T. W. Measurements and Modeling of Recombination from Nanoparticle TiO_2 Electrodes. *J. Am. Chem. Soc.* **2011**, *133*, 8264−8271.
(70) Kalb, W. L.; Haas, S.; Krellner, C.; Mathis, Th.; Batlogg, B. Trap Density of States in Small-Molecule Organic Semiconductors: A Quantitative Comparison of Thin-Film Transistors with Single Crystals. *Phys. Rev. B* **2010**, *81*, 155315.
(71) Salleo, A.; Chen, T. W.; Völkel, A. R.; Wu, Y.; Liu, P.; Ong, B. S.; Street, R. A. Intrinsic Hole Mobility and Trapping in a Regioregular Poly(thiophene). *Phys. Rev. B* **2004**, *70*, 115311.
(72) Anta, J. A.; Mora-Sero, I.; Dittrich, T. Dynamics of Charge Separation and Trap-Limited Electron Transport in TiO_2 Nanostructures. *J. Phys. Chem. C* **2007**, *111*, 13997−14000.
(73) Anta, J. A.; Idigoras, J.; Guillen, E.; Villanueva-Cab, J.; Mandujano-Ramirez, H. J.; Oskam, G.; Pelleja, L.; Palomares, E. A Continuity Equation for the Simulation of the Current−Voltage Curve and the Time-Dependent Properties of Dye-Sensitized Solar Cells. *Phys. Chem. Chem. Phys.* **2012**, *14*, 10285−10299.
(74) Shi, Y. S.; Dong, X. D. Coupled Analysis of Steady-State and Dynamic Characteristics of Dye-Sensitized Solar Cells for Determination of Conduction Band Movement and Recombination Parameters. *Phys. Chem. Chem. Phys.* **2013**, *15*, 299−306.
(75) Jennings, J. R.; Wang, Q. Influence of Lithium Ion Concentration on Electron Injection, Transport, and Recombination in Dye-Sensitized Solar Cells. *J. Phys. Chem. C* **2010**, *114*, 1715−1724.
(76) Coehoorn, R.; Bobbert, P. A. Effects of Gaussian Disorder on Charge Carrier Transport and Recombination in Organic Semiconductors. *Phys. Status Solidi A* **2012**, *209*, 2354−2377.
(77) Arkhipov, V. I.; Heremans, P.; Adriaenssens, G. J. Space-Charge-Limited Currents in Materials with Gaussian Energy Distributions of Localized States. *Appl. Phys. Lett.* **2001**, *79*, 4154.
(78) Anta, J. A.; Mora-Sero, I.; Dittrich, T.; Bisquert, J. Interpretation of Diffusion Coefficients in Nanostructured Materials from Random Walk Numerical Simulation. *Phys. Chem. Chem. Phys.* **2008**, *10*, 4478−4485.
(79) Jansson, F. *Charge Transport in Disordered Materials; Simulations, Theory, and Numerical Modeling of Hopping Transport and Electron-Hole Recombination*. Ph.D. Thesis, Åbo Akademi University, 2011.
(80) Fishchuk, I. I.; Kadashchuk, A.; Bässler, H.; Abkowitz, M. Low-Field Charge-Carrier Hopping Transport in Energetically and Positionally Disordered Organic Materials. *Phys. Rev. B* **2004**, *70*, 245212.
(81) Anta, J. A.; Nelson, J.; Quirke, N. Charge Transport Model for Disordered Materials: Application to Sensitized TiO_2. *Phys. Rev. B* **2002**, *65*, 125324.
(82) Mendels, D.; Tessler, N. Drift and Diffusion in Disordered Organic Semiconductors: The Role of Charge Density and Charge Energy Transport. *J. Phys. Chem. C* **2013**, *117*, 3287−3293.
(83) Vaynzof, Y.; Preezant, Y.; Tessler, N. Current Voltage Relation of Amorphous Materials Based on Diodes-The Effect of Degeneracy in Organic Polymers/Molecules. *J. Appl. Phys.* **2009**, *106*, 084503.
(84) Sun, Z.; Zhang, R.; Xie, H.; Wang, H.; Liang, M.; Xue, S. Nonideal Charge Recombination and Conduction Band Edge Shifts in Dye-Sensitized Solar Cells Based on Adsorbent Doped Poly(ethylene oxide) Electrolytes. *J. Phys. Chem. C* **2013**, *117*, 4364−4373.
(85) Kopidakis, N.; Benkstein, K. D.; van de Lagemaat, J.; Frank, A. J. Transport-Limited Recombination of Photocarriers in Dye-Sensitized Nanocrystalline TiO_2 Solar Cells. *J. Phys. Chem. B* **2003**, *107*, 11307−11315.
(86) Anta, J. A.; Casanueva, F.; Oskam, G. A Numerical Model for Charge Transport and Recombination in Dye-Sensitized Solar Cells. *J. Phys. Chem. B* **2006**, *110*, 5372−5378.
(87) Villanueva-Cab, J.; Oskam, G.; Anta, J. A. A Simple Numerical Model for the Charge Transport and Recombination Properties of Dye-Sensitized Solar Cells: A Comparison of Transport-Limited and Transfer-Limited Recombination. *Sol. Energy Mater. Sol. Cells* **2010**, *94*, 45−50.
(88) Petrozza, A.; Groves, C.; Snaith, H. J. Electron Transport and Recombination in Dye-Sensitized Mesoporous TiO_2 Probed by Photoinduced Charge-Conductivity Modulation Spectroscopy with Monte Carlo Modeling. *J. Am. Chem. Soc.* **2008**, *130*, 12912−12920.

(89) ben-Avraham, D.; Havlin, S. *Diffusion and Reactions in Fractals and Disordered Systems*; Cambridge University Press: Cambridge, U.K., 2000.
(90) Méndez, V.; Fedotov, S.; Horsthemke, W. *Reaction-Transport Systems*; Springer-Verlag: Berlin Heidelberg, 2010.